PROCEEDINGS OF SPIE

SPIEDigitalLibrary.org/conference-proceedings-of-spie

Optical estimation of fractal dimension for image assessment

Samuel Peter Kozaitis
Rufus H. Cofer

SPIE.

Optical Estimation of Fractal Dimension for Image Assessment

S. P. Kozaitis, R. H. Cofer

Florida Institute of Technology,
Department of Electrical and Computer Engineering
Melbourne, FL 32901-6988

ABSTRACT

We modeled an optical system for estimation of the fractal dimension to provide a measure of surface roughness for an entire image and for image segmentation. Although the simulated optical result was similar to that calculated by digital techniques, both suffered from problems encountered known to occur with estimating fractal dimension. Furthermore, the optical estimation did not have as good as resolution of that obtained with digital estimates due primarily to the limited dynamic range of the detector.

1 INTRODUCTION

Numerical techniques have been used to estimate the dimension of fractal objects.[1] Although there are a variety of practical issues associated with making a estimation from finite data, others have shown that fractals may be well-suited to some signal processing applications. For example, the estimation of fractal dimension has been used to perform texture segmentation and classification in images using natural terrain.[2]

Optical techniques have been explored to perform segmentation in imagery because of the potential high speed available through the Fourier transforming property of a lens.[3] We explore segmentation by estimating the fractal dimension from an optically generated power spectrum. Although several algorithms have been used to estimated the fractal dimension, the power spectrum technique[4] is one that is well-suited to optics. In the next section we briefly discuss the fractal dimension, in following sections we describe the model of our optical system following some sources of error that are possible. Finally, we describe segmentation results and discuss our conclusions.

2 FRACTAL DIMENSION

In one topological dimension, a Fractal Brownian line function $B_H(t)$ with a Fourier power spectrum $F_H(f)$ may be described as[5]

$$F_H(f) \propto f^{-B} \tag{1}$$

and H is related to B by

$$B = 2H + 1 \tag{2}$$

and to the fractal dimension D of $B_H(t)$ by

 0-8194-0867-0/92/$4.00

$$D = 2 - H. \tag{3}$$

The form of a power spectrum of a fractal function is shown in Fig. 1. In two topological dimensions, a Fractal Brownian surface function $B_H(x,y)$ with a Fourier power spectrum $F_H(f,\theta)$ may be described as[5,6]

$$F_H(f,\theta) \propto f^{-B} \tag{4}$$

where

$$B = 2H + 2. \tag{5}$$

A slice through the surface $B_H(x,y)$ is a Fractal Brownian line function of identical H.[5]

Figure 1 Typical power spectrum of a fractal

3 OPTICAL SYSTEM

We considered a basic Fourier optical system for our model like that shown in Fig. 2. Here, collimated light illuminates a spatial light modulator (SLM) whose Fourier transform is generated by the lens. We modeled the effects due the limited dynamic range of a detector, finite pixel size of the SLM, and nonuniform intensity distribution of an incident Gaussian beam. Using this model, we considered our system a rough lower bound of performance. We compared our results to a digital representation using 32-bit floating point data. We considered the results of the latter system a rough upper bound of the optical system.

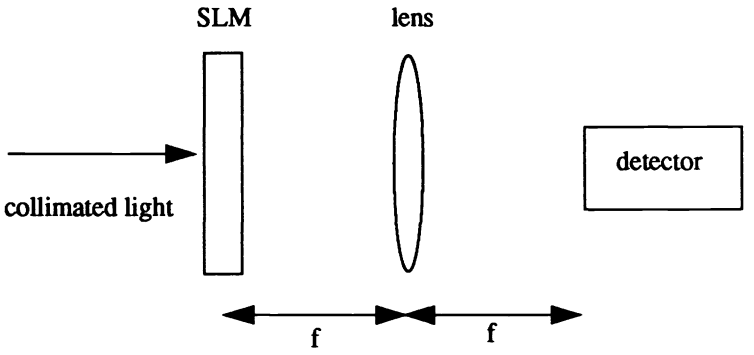

Figure 2 Schematic diagram of optical set-up

3.1 Dynamic range

Although discretization is a source of error in estimating fractal dimension, the limited dynamic range of many optical detectors may increase the error. With a digital system, many orders of magnitude of values can be represented in floating point form. With an optical detector such as a camera, the dynamic range is often smaller. In addition, the useful dynamic range of a detector would be affected by the DC value of the power spectrum. When the power spectrum was normalized, the intensity in the vicinity of the DC was often much greater than at other frequencies. Therefore, the value of intensity at frequencies other than the vicinity of the DC would be measured to be near 0. To eliminate this effect, we blocked a region in the vicinity of the DC. The extent of the DC spot will have a minimum value determined from the diffraction-limited effect of the lens. In addition, a bias was also added to the detector response so that the detector intensity was never 0.

We modeled our detector as linear with 8-bit resolution. The resolution affected the quantization of the vertical scale in Fig. 1 with a greater affect toward the higher frequencies. At some point the intensity would be lower than the lowest quantization level of the detector; therefore, to yield reasonable estimates of the slope of the power spectrum, the range of frequencies had to be limited.

3.2 Intensity distribution

When an image is displayed on a spatial light modulator (SLM) and illuminated by a laser, the intensity across the SLM will not be constant. The intensity of the beam with a planar wavefront will likely have a Gaussian shape according to[7]

$$I(r) = I_0 exp\left[\frac{-2r^2}{w_0^2}\right] \tag{6}$$

where r is the variable in the radial direction and w_0 is the spot size of the beam. The effect of this nonuniform distribution was that the power spectrum was convolved with a Gaussian function. As the input beam

became less uniform, the power spectrum was convolved with a broader function.

3.3 Pixel size

The finite size of the pixels of an SLM will affect the power spectrum by diffraction. Neglecting the finite extent of the SLM with all the pixels set to "1," the SLM was represented as a pixel convolved with a sampling grid as[8]

$$h(x, y) = \frac{1}{d^2} comb\left(\left(\frac{x}{d}, \frac{y}{d}\right) \otimes rect\left(\frac{x}{w}, \frac{y}{w}\right)\right) \tag{7}$$

where $\otimes$ indicates convolution, w is the width of a pixel of the SLM and x and y are continuous variables in the input plane. The Fourier transform of Eq. (6) yields a *sinc* function multiplied by the Fourier Transform of the input image.

4 SEGMENTATION

Segmenting an image using digital techniques by 8 x 8 pixel regions using estimates of the fractal dimension has been previously considered.[2] We considered the same situation using a system similar to that of Fig. 1 to simulate optical segmentation. In this case, the lens in Fig. 2 would be replaced by an array of lenses. Although lenses usually have a circular cross-section and pixels are often square, some pixels may be missed in the optical implementation; however, we neglected this effect.

We used several images to simulate optical fractal dimension estimates and compared those results with a digital implementation using the power spectrum technique. We found that digital techniques could be used to obtain different slopes for a line like that in Fig. 1. Images of similar roughness had relatively stable slopes and those surfaces with a differing roughness generally gave different slopes.

The optical simulations were modeled with an 8-bit linear detector, spacing between pixels of 20% the length of a pixel, and a Gaussian beam with intensity at the edge of the image of 50% that of the center.The results were similar to the digital results but the were unable to detect small changes in slope. A 256 x 256 image used in our experiments is shown in Fig. 3. The histograms of the segmented image using digital and optical techniques are shown in Figs. 4(a-b) respectively. Although both methods produced a similar range of slopes, the slopes generated using the optical method seemed to be mixed together to some degree.

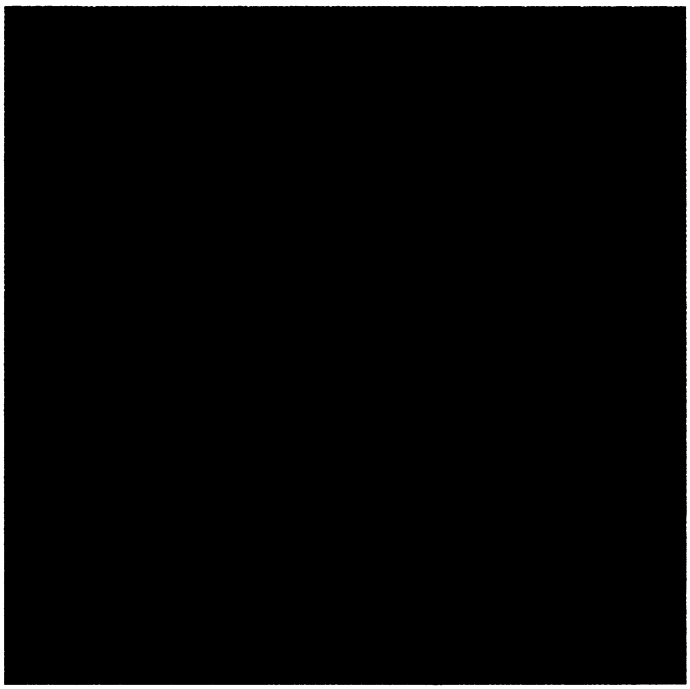

Figure 3 An image used in our simulations

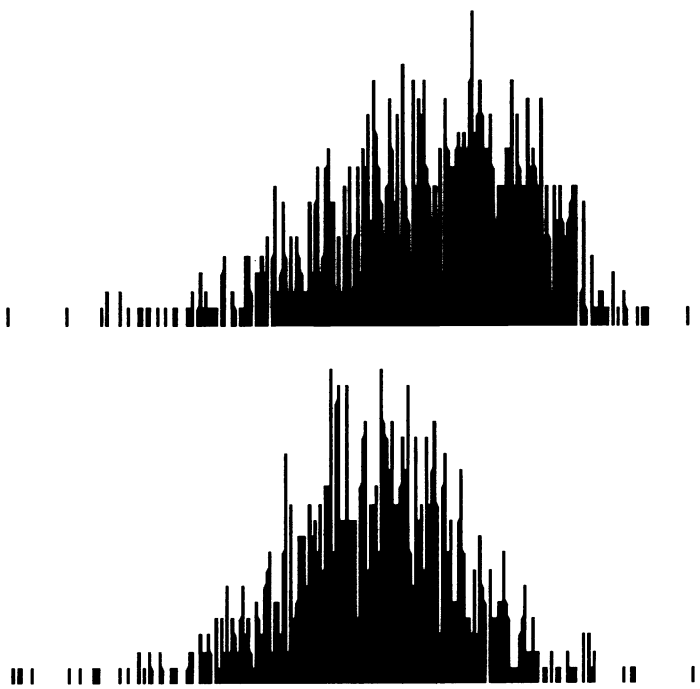

Figure 4 Histograms of image in Fig. 3 after segmentation (top image is for digital result, bottom is for simulated optical).

5 SUMMARY AND CONCLUSIONS

We modeled an optical system for estimation of the fractal dimension to provide a measure of surface roughness for an entire image or image segmentation. Although the simulated optical result was similar to that calculated by digital techniques, they both suffered from problems known to occur when estimating fractal dimension. The optical estimation did not have as good as resolution of that obtained with digital estimates due primarily to the limited dynamic range of the detector.

6 REFERENCES

[1] J. Theiller, "Estimating fractal dimension," *Jour. Opt. Soc. Amer. A* vol. 7(6), 1055-1073 (1990)

[2] A. Pentland, "Fractal-based description of natural scenes," *IEEE Trans. Pattern Anal. Machine Intell.*, vol PAMI-6(6), 661-674 (1984)

[3] C. P. Veronin, K. L. Priddy, S. K. Rogers, K. W. Ayer, M. Kabrisky, and B. Welsh, "Optical image segmentation using neural-based wavelet filtering techniques," *Optical Engineering* vol 31(2), 287-293 (1992)

[4] B. B. Mandelbrot, and J. Van Ness, "Fractional brownian motions, fractional noises and applications," *SIAM Rev.* vol. 10(4) 422 (1968)

[5] P. Kube, and A. Pentland, "On the imaging of fractal surfaces," *IEEE Trans. Pattern Anal. Machine Intell.*, vol PAMI-10(5), 704-707 (1988)

[6] R. F. Voss, "Random fractal forgeries," in *Fundamental Algorithms for Computer Graphics*, R. A. Earnshaw, Ed. Berlin: Springer-Verlag, 1985

[7] J. T. Verdeyen, Laser Electronics, Prentice Hall: New Jersey (1989)

[8] B. D. Bock, T. A. Crow, and M. K. Giles, "Design considerations for miniature optical correlation systems that use pixelated input and filter transducers," *Optical Information Processing Systems and Architectures II*, B. Javidi, Ed., Proc. SPIE 1347, 297-309 (1990)